Science of Sintering, **55** (2023) 89-101

https://doi.org/10.2298/SOS2301089S

UDK: 669.14; 622.785

The Effect of Insert Surface Roughness in Part Production with Inserted Powder Injection Molding Method

Kamran Samet[1], Mehmet Subaşı[2*)], Çetin Karataş[3]

[1]Gazi University, Faculty of Technology, Manufacturing Engineering, Turkish Aerospace, Ankara, Turkey

[2]Technical Sciences Vocational School of Higher Education, Gazi University, Ankara, Turkey

[3]Gazi University, Faculty of Technology, Manufacturing Engineering, Ankara, Turkey

Abstract:

The Powder Injection Molding (PIM) method is widely used in the production of parts with complex geometries and small volumes. To solve the volume limitation in PIM, the Inserted Powder Injection Molding (IPIM) method was developed. In this study, the effect of insert surface roughness on shear strength was investigated using the IPIM method in the production of WC-9%Co parts. Firstly, inserts with five different surface roughness (Ra, µm), 1.5 - 2.1 - 3.3 - 4 - 4.6, were prepared from 4340 steel for the research. WC feedstock was injected onto the prepared inserts. Following the injection process, the samples were subjected to debinding and sintering processes. Compression tests were performed on sintered specimens, and the effect of surface roughness on diffusion bonding strength was investigated. As a result of the experiments, it was determined that the shear strength increases with the increase of the insert surface roughness. The maximum shear strength (118.4 MPa) was obtained in samples with an insert surface roughness of 4.6 µm.

Keywords: *Inserted Powder Injection Molding; Surface roughness; Diffusion bonding; Shear strength; WC feedstock.*

1. Introduction

Because of its excellent hardness and wear resistance values, tungsten carbide (WC) is a preferred material in engineering applications. Because of this, research on reinforced WC's [1] and hybrid composite materials is growing steadily [2,3].

Powder Injection Molding (PIM) consists of four basic steps: feedstock preparation, moulding, debinding, and sintering [4]. The PIM is the preferred method for producing complex shaped and small parts. Additionally, it is employed in the manufacture of numerous components, including medical screws [5], which must be biocompatible [6].

The PIM process is similar to the plastic injection molding method in several aspects. However, in the PIM method, the part thickness should not be greater than 10 mm [7,8]. The IPIM method was created to overcome this constraint in the production of parts with PIM. The IPIM process begins with the preparation of inserts, followed by the injection of feedstock onto the inserts. After the injection of the feedstock onto the insert, the samples are

*) **Corresponding author:** msubasi@gazi.edu.tr (M.Subaşı)

subjected to debinding and sintering processes. The ability to produce parts thicker than 10 mm from different materials is the most significant advantage of the IPIM method.

Surface roughness is the sum of irregularities such as cutting tool marks, faults, and waves that occur on the surface of the part depending on the manufacturing technique. Surface roughness is a critical parameter influencing part quality [9-11]. Many studies have been carried out to assess the effect of surface roughness on diffusion welding [12-15]. According to Li et al. [16] low surface roughness was efficient in diffusion welding, and plastic deformation (creep) became more effective as the roughness increased. The join mechanism of the insert and the feedstock in the IPIM method is the same as in diffusion welding. Surface roughness is a significant factor influencing join strength in diffusion welding. The fact that the surface roughness is not optimum, a gap occurs between the two joined regions, resulting in weak bond strength [17-19]. The use of intermediate layers in diffusion welding applications is a commonly used technique to increase the mechanical properties of the joint [20-22]. There are different studies in the literature conducted with IPIM and the co-injection method. Safarian et al. [23] investigated the producibility of IPIM method parts using 316L insert and feedstock. It is found that the sintering temperature and the insert/part diameter ratio are significant parameters in the IPIM method as a result of that research. Koçak et al. [24] investigated the effect of using an interlayer in the production of WC parts using the IPIM method. As a result of the experiments, it is found that using an intermediate layer in the IPIM method increases the diffusion between the feedstock and insert regions. Subaşı [25] investigated the effect of interlayer thickness on the insert in the production of parts from 316L feedstock with the IPIM method. As a consequence of the experiments, it was observed that increasing the thickness of the intermediate layer has a beneficial effect on bond strength. Dourandish et al. [26] in their research of the joining of zirconia and stainless steel parts, revealed that the materials' thermal expansion coefficients are important parameters. Firouzdor et al.[27] tried to create a hybrid structure out of high speed steel (HSS) and 17-4 PH stainless steel materials. In this research, it is determined that the sintering temperature is a critical factor in increasing the joint surface. Johnson et al. [28] studied the production of a cylinder geometry part out of stainless steel and alumina materials. It is determined that the part thickness and shrinkage ratio of the materials should be as equal as possible in order to maximize the diffusion bond between these two materials. Li et al.[29] investigated the producibility of a part with a cylinder geometry, inner and outer parts of which are tungsten carbide material, by co-injection method. As a result of the experiments, it is determined that atomic transitions between two regions improve the mechanical properties of diffusion in the intermediate region.

In this study, the effect of insert surface roughness on the joining between regions was studied using the IPIM method on the producibility of a part with an inner part of 4340 steel and an outer part of WC-9% Co. Firstly, inserts with different surface roughness (1.5-2.1-3.3 – 4-4.6 μm) were prepared for the experiments. These inserts were injected with WC feedstock. After injecting of the feedstock, the samples were subjected to debinding and sintering processes. Then, the samples were subjected to compression tests. As a result of these experiments, the effect of insert surface roughness on diffusion bonding strength was investigated.

2. Materials and Experimental Procedures

2.1 Feedstock

The WC-9%Co feedstock used in the study was supplied as a commercial product from the RYER Inc. Spectral analysis values and technical specifications of the feedstock are given in Table I and Table II, respectively.

Tab. I Chemical composition of WC-Co feedstock.

Elements	**C**	**Cr**	**Fe**	**Mo**	**Ni**	**W**	**Co**	**O**
Wt %	5.54	0.01	0.01	0.01	0.01	85.43	8.94	0.05

Tab. II Technical properties of WC-Co feedstock.

Powder shape	**Density**	**Powder size(μm)**		
		D10	D50	D90
Complex shaped	8.06 g/cm³	0.15	0.28	0.52

2.2 Insert material and surface roughness

The material and geometry of the insert is an important parameter in part production with the IPIM method. In this study, the inserts used in the preparation of the research samples were made from 4340 steel material (Fig. 1). Inserts were machined in five different average surface roughness as 1.5-2.1-3.3 – 4-4.6 µm. The surface roughness values of the machined inserts were determined using a surface roughness measuring device (Mahr Perthometer M1). At least three measurements were realized and averaged for grouping the surface roughness of inserts.

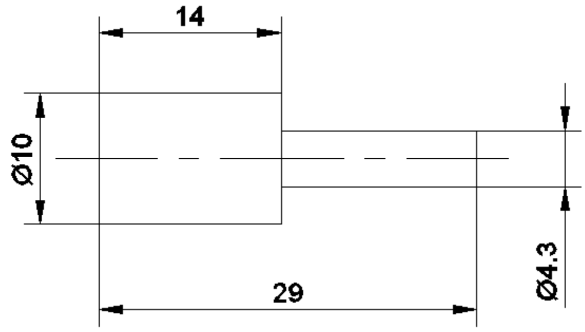

Fig. 1. Dimensions of the insert (mm).

2.3 Injection parameters

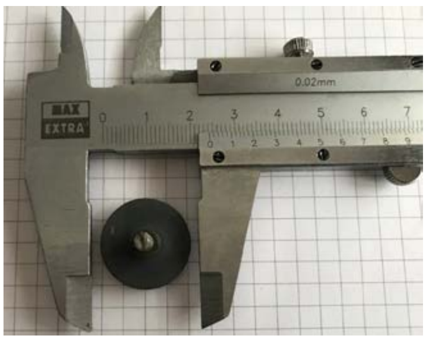

Fig. 2. A sample prepared with the IPIM method.

In order to inject the test samples, an Arburg Allrounder 220 S/250-60 injection machine was used. Injection parameters used in sample preparation with the IPIM method are given in Table III. The sample after injection process is shown in Fig. 2.

Tab. III The sample preparation parameters with the IPIM method.

Injection rate (cm^3/s)	Injection pressure (bar)	Injection time (s)	Holding pressure (bar)	Injection temperature (°C)	Mold temperature (°C)	Cooling time (s)
15	1000	2	80	200	45	5

2.4 Debinding process

Chemical debinding was applied to the samples after the injection molding process. The chemical debinding experiments of the samples were carried out by keeping them in ethanol at 60°C for 48 hours.

2.5 Thermal debinding and sintering process

After the chemical debinding process, the samples were subjected to thermal debinding and sintering in the same process. Thermal debinding and sintering processes were carried out in a control atmosphere tube furnace using 5% hydrogen + 95% nitrogen gas mixture.

Thermogravimetric (TG) analysis was performed to determine the parameters of the thermal debinding process and the temperatures at which the samples lost mass (Fig. 3). As a result of TG analysis, it was determined that 5.24 % of the binders were separated from the sample between 175-475°C, and after 475°C there was no significant loss of mass until the sintering temperature. According to the TG analysis, the thermal debinding stage and sintering cycle were determined by decreasing the temperature increase rate at temperatures with excessive mass losses (Fig. 4). Sintering experiments were carried out at 1300°C for 240 minutes.

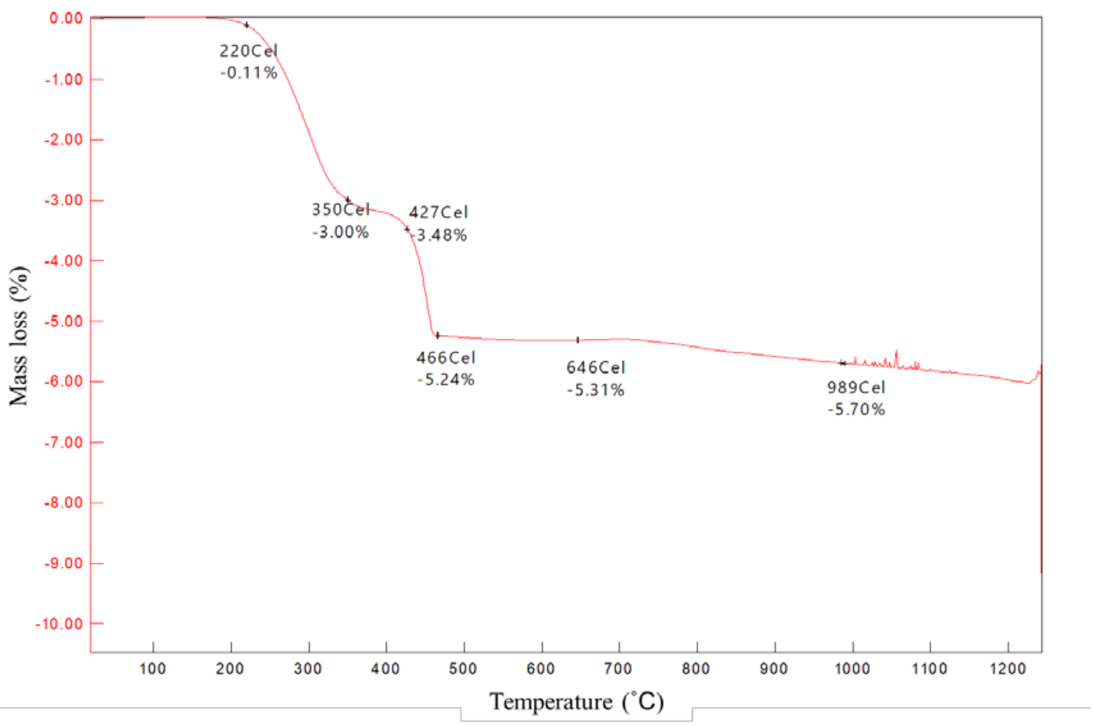

Fig. 3. Mass losses as a result of TG analysis.

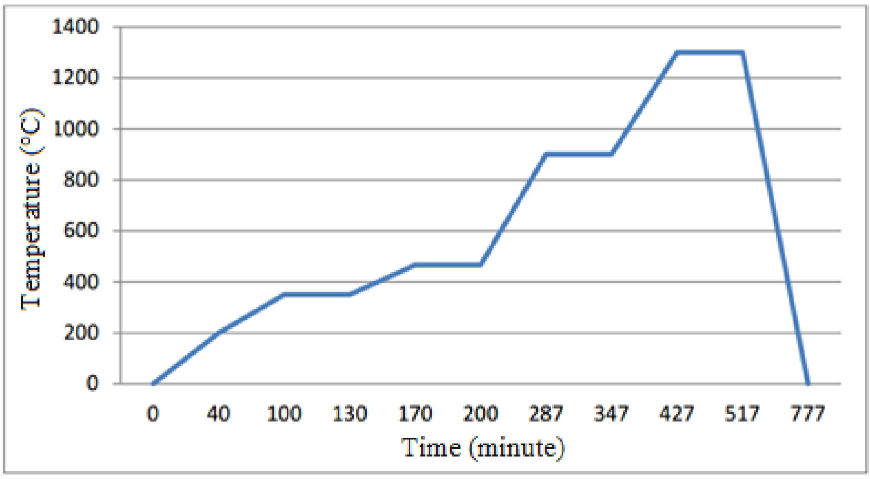

Fig. 4. Thermal debinding and sintering cycle.

2.6 Metallographic and mechanical tests

Metallography tests were carried out to reveal and examine the internal structure of the test samples. The surfaces were sanded with six separate sandpapers during the metallography analyses, the last of which was 1200 grit. Subsequently, the samples were etched with 1% nital + distilled water mixture after sanding. The internal structure images of the samples were examined using Jeol JEM 6060 LV Scanning Electron Microscope (SEM). Mechanical tests were carried out on a 50 kN capacity Instron brand compression tensile device regarding of the TSE 206 standard. Compression tests were performed on three different samples, and the results were averaged.

The equations mentioned below are used to calculate shear strength. In the equations used in the calculations, D_i diameter (mm), t_e thickness (mm) (Fig. 5), P_b is the compression force (kN).

$$A_d = \pi D_i t_e \quad (1)$$

$$\tau = \frac{P_b}{A_d} \quad (2)$$

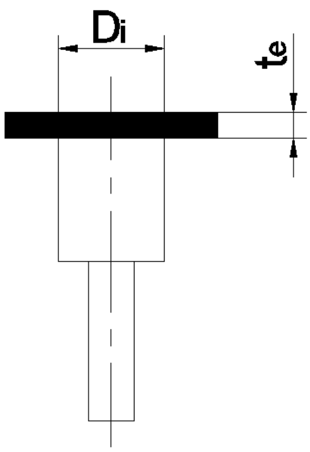

Fig. 5. Dimensions used for calculating shear strength.

3. Results and Discussion

In this study, the effect of insert surface roughness on diffusion bonding strength was investigated in the production of WC-9%Co with inserts by the IPIM method. The samples prepared using the IPIM method consist of 4340 steel in the inner part and WC-9%Co feedstock in the outer part. The join strength, which occurs as a result of diffusion between the feedstock and the insert having different surface roughness, was determined by a compression strength test. The shear strength of the inserted samples was calculated using the maximum compression force obtained from the tests. As a result of the calculations made using Equation 1 and 2, the average shear strength values given in Table IV were obtained. Fig. 6 demonstrates the WC feedstock diffused onto the insert surface of sintered sample. The compression test graph of the sample, which has the insert average surface roughness value of 2.1 μm and was sintered at 1300°C in 240 minutes, is given in Fig. 7. As a result of the experiments, it was determined that the shear strength value increases with the increase in the surface roughness value (Fig. 8). It is thought that the increase in shear strength with the increase in the surface roughness value is related to the wavelength (λ) and height (H) of the surface roughness.

Tab. IV Average shear strength results.

	Average surface roughness (R_a, µm)				
	1.5	2.1	3.3	4	4.6
Average shear strength(MPa)	67.76	93.33	97.72	108.8	118.4

Fig. 6. The WC feedstock diffused onto the insert surface after the compression test.

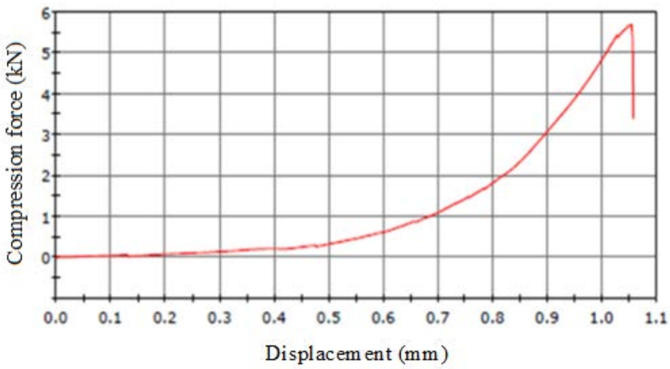

Fig. 7. Compression test graphic of the inserted sample sintered at 1300°C for 240 minutes.

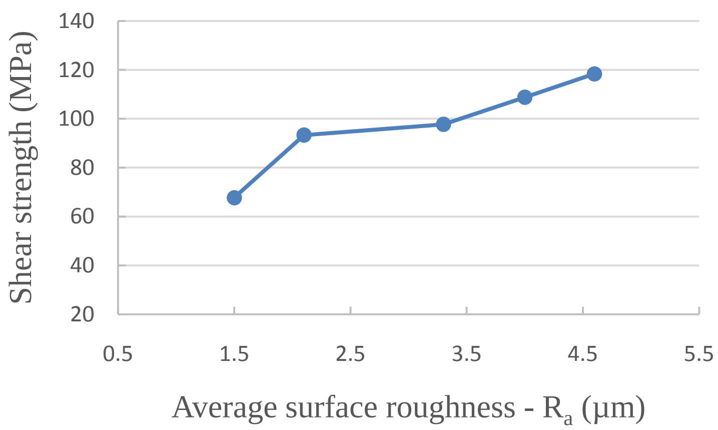

Fig. 8. The effect of insert surface roughness on shear strength.

The wavelength (λ) and height (H) of the surface roughness are two parameters that determine the average surface roughness value. Fig. 9a shows surface roughness at a fixed length (L) and the same wavelength, while Fig. 9b shows surface roughness of the same height at a fixed length. In both parameters, it was determined that as the surface roughness value increased, the amount of powder particles attached to the insert surface increased due to the increase in the insert surface area. When the wavelength is kept constant, it is determined the number of powder particles sticking to the surface at the lowest surface roughness value is 75 (a), while the number of powder particles sticking to the surface as the surface roughness increases is 77 (b), 97 (c), and 128 (d), respectively (Fig. 9a). When the height of the insert surface roughness is kept constant, it is determined that the 75 (a), 83 (b), 93 (c), and 128 (d) powder were attached to surface (Fig. 9b). It is determined that for the surface roughness at constant wavelength and constant height, the number of powder particles attached to the insert surface is close.

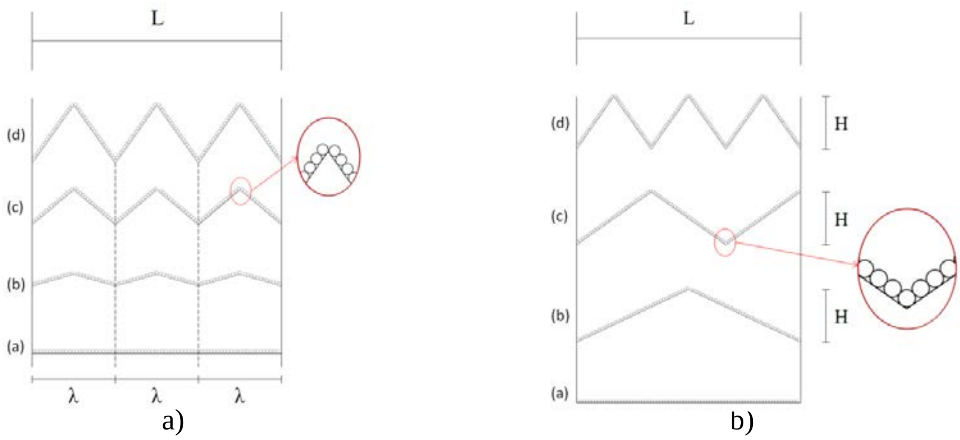

Fig. 9. The average surface roughness value's wavelength (λ) and height (H): a) Surface roughness at a fixed length (L) and the same wavelength b) Surface roughness of the same height at a fixed length (L).

According to the results, increasing the amount of powders attaching to the insert surface during sintering increases the bond strength (Fig. 8). As a result, the increase in contact surface area between the inner (4340 steel) and outer (WC-9%Co) regions is thought to improve diffusion between the two regions. Therefore, higher compression force was measured for the samples with high average surface roughness in the compression test. It was reported in a study of super alloy materials joined by diffusion welding that the bond strength increased as the surface roughness value decreased [13]. In another study using diffusion welding to join WC-Co and 40Cr steels, it was reported that bond strength increased on surfaces with low surface roughness values [12]. Many studies exploring the effect of surface roughness value on joining (diffusion) obtained similar results [14,31,32]. However, when the studies were examined, it was determined that the experiments were carried out with rolling material. As exposed to high temperature and pressure, rolled materials behave differently than powder-based materials. In a different study on diffusion welding, it is stated that surface roughness deforms under pressure [33]. Furthermore, under high temperature and pressure, in a specific period of time, the surface asperities are changed their shape by subjecting creep deformation (Fig. 10). As the materials to be joined reach the glassy transition temperature at high temperatures in the diffusion welding process, the asperities on the surface of the materials are changed their shape under the effect of pressure. With the pressure applied during the joining process, the roughness decreases and surfaces with low surface roughness are formed. For this reason, when joining the roll materials with diffusion welding, the surface area of the contact regions can be increased by decreasing the roughness values of the joining area. Thus, high bonding strength can be obtained with smoother surfaces.

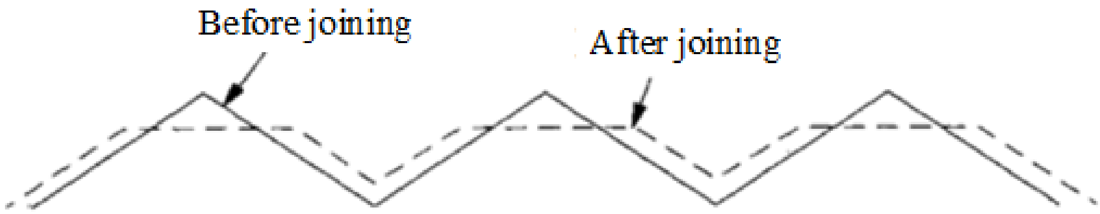

Fig. 10. Deformation of surface roughness in the diffusion welding method.

Although the increase in the surface roughness value in joints where rolling materials are used has a weakening effect on the diffusion welding, it has a positive effect on powder-based materials, such as feedstock. The reason for that, depending on the increase in the surface roughness on the insert, a larger surface area of the injected feedstock can come into contact with the insert. As a result, with the increase in the surface roughness of the insert, the number of powders that can be attached to the insert surface increases.

3.1. Evaluation of the Diffusion Region

In previous studies, interlayers were used to achieve the targeted joining or to shorten the diffusion time [12,34-37]. Wang et al.[38] used a silicon nitrate interlayer to join titanium and ceramic materials without any problems. As a result, they were able to obtain a proper joining surface. Nicholas and Crispin [39] investigated the impact of interlayer on shear strength in the joining of stainless steel and alumina. As a result of the experiments, shear strength of 29.5 MPa is obtained for the samples without interlayer, while shear strength of 70 MPa is obtained for the samples using aluminum interlayer.

Zhao and Zhang [40] investigated the effect of the interlayer on diffusion of magnesium and aluminum materials. While 41.3 MPa shear strength is obtained in test samples without interlayer, it is determined 83 MPa shear strength in test samples with zinc interlayer. In this study, the average shear strength of 97.21 MPa was obtained as a result of the experiments. It has been determined that this value is higher than the shear strength value obtained results of many studies using interlayer in the literature.

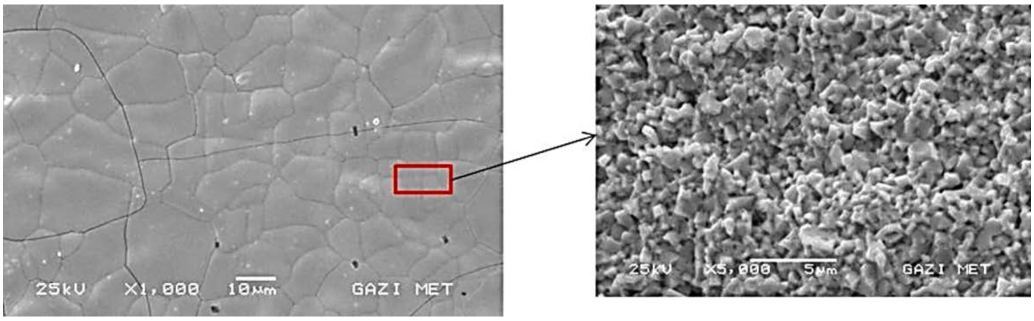

Fig. 11. SEM image of the sample sintered at 1300°C for 240 minutes (feedstock region).

The scanning electron microscopy (SEM) was used to characterize the microstructure of the bonding interface and feedstock region. It was observed that the powder grains of the samples sintered at 1300°C for 240 minutes were tightly packed. It was also observed that the grain structure has become clear (Fig. 11). The SEM images display that there is a void-free structure on the contact area of the parts, and the join (diffusion) was generated successfully (Fig. 12).

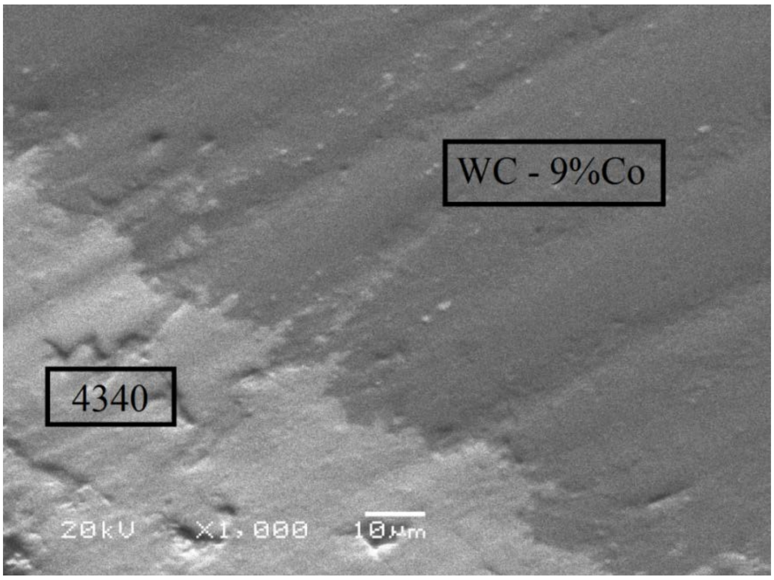

Fig. 12. Feedstock (WC-9% Co) and insert (4340 steel) diffusion region.

After examining the diffusion region with SEM, Energy Dispersion Spectroscopy (EDS) analyses were performed to determine the changes in the chemical composition of the elements between the insert and feedstock regions (Fig. 13).

According to the results of the EDS analysis, the concentration changes between the insert and feedstock regions are shown in Fig. 14. According to EDS analysis, it has been understood that the four main elements (tungsten, cobalt, nickel, and iron) provide joining (diffusion).These elements provided the joining by diffusing to the opposite area during sintering. According to the results of the analysis, it was observed that the iron (Fe), which is abundant in 4340 steel, has diffusion up to approximately 600 µm towards the injection area. The nickel (Ni) was determined to diffuse up to 350 µm towards the feedstock region (Point 3). For the reverse direction, tungsten (W) and cobalt (Co) carried out the diffusion towards the insert region. As a result of the analysis, it was observed that tungsten and cobalt atoms diffused more than 400 µm towards the insert region.

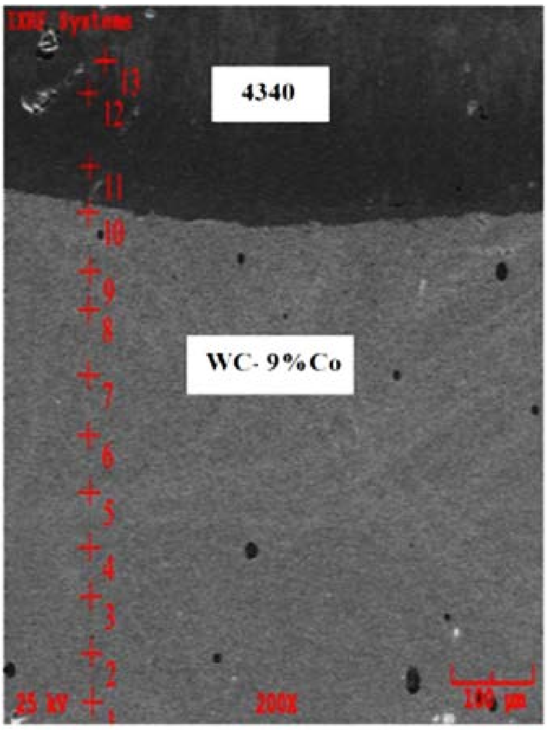

Fig. 13. Points of EDS analysis between the insert and feedstock regions.

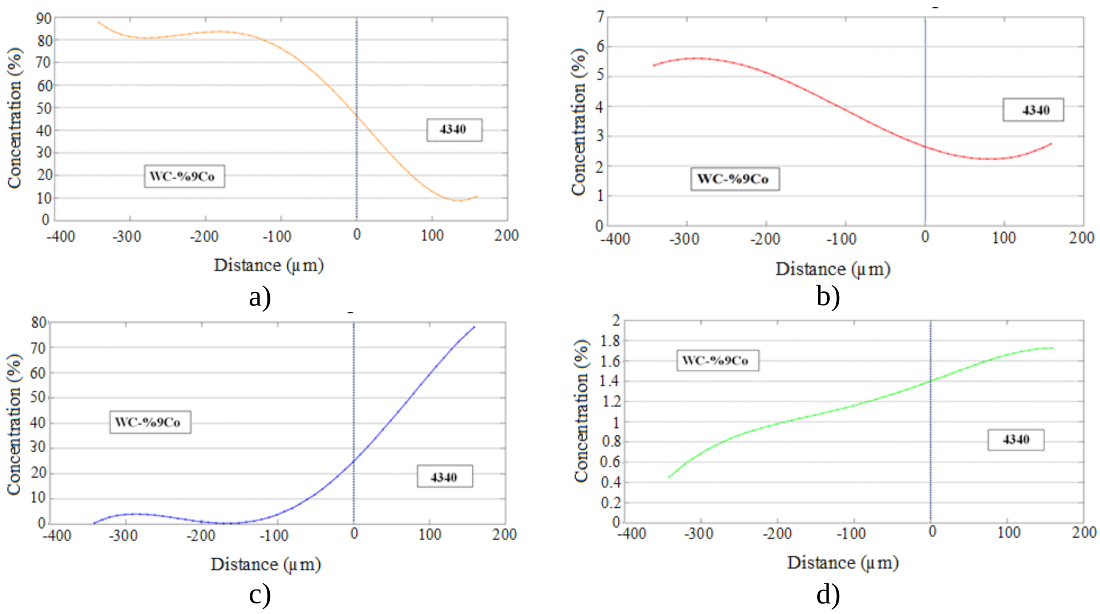

Fig. 14. Concentration changes of elements between the insert and feedstock regions: a) Tungsten concentration changes b) Cobalt concentration changes c) Iron concentration changes d) Nickel concentration changes.

3.2. Microhardness analysis

The microhardness profile in the diffusion region of the samples sintered at 1300°C with 240 minutes holding time is given in Fig. 15. According to the hardness measurement results, the average hardness of the insert region is 416 $HV_{0.2}$. For the injected region the average hardness was calculated as 1590 $HV_{0.2}$. It can be seen that the average hardness value of the injected side (WC-9%Co) is lower than the reference WC hardness values for the joining region. This can be explained as follow, elements passing from the insert region (4340) to the injected region reduce the hardness of the region (injected region). However, it is worth noting that, as we move away from the interface hardness profile of the injected region increases.

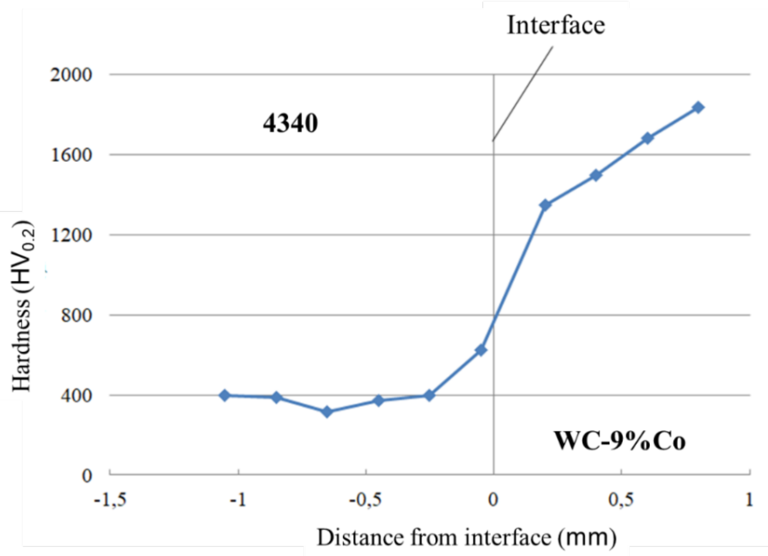

Fig. 15. Microhardness profile for the joining region.

4. Conclusion

Results from this study have led to a deeper understanding about how effects the insert (4340 steel) surface roughness to diffusion bonding strength for WC parts prepared by using IPIM method. Main results obtained from this study are as follows:

- The insert surface roughness of the samples is a parameter that influences the bonding strength for IPIM method.
- It was determined that increasing the roughness of the insert surface increases diffusion bonding strength. The highest shear strength was obtained for samples with an insert average surface roughness of 4.6 µm (118.45 MPa), while the minimum shear strength was obtained for samples with an insert average surface roughness of 1.5 µm (67.76 MPa).
- The average of the shear strength values obtained for different surface roughness is 97.21 MPa.
- According to the EDS analysis of the joining region W, Co, Fe, Ni are the main elements that provide the diffusion between inner (insert region) and outer part (injection region) of the samples.
- As a result of the sintering experiments, it was determined that Ni diffuses up to 350 µm into the outer part and Co diffuses approximately 400 µm to the inner part.
- When the microhardness measurement results are examined, it can be easily observed that the hardness value increases at the transition from the inner part to the outer part of the samples. Joining region has a hardness value that is between the hardness of the inner part (4340 steel) and the outer part (WC).

Acknowledgments

This research was sponsored by the Scientific and Technological Research Council of Turkey (TÜBITAK), Project No: 115M437 and Gazi University Research Funds, Project No: 07/2016-21. The authors would like to express their sincere appreciation to TÜBITAK organization and Gazi University for their financial supports.

5. References

1. M. Akkaş, F.R.A.A.Sudani, Science of Sintering, 53, (2021) 19-35.
2. Z. Özkan, H. Gökmeşe, U. Gökmen, Science of Sintering, 54, (2022) 177-187.
3. S. Filipović, N. Obradović, Lj. Andjelković, et al. Science of Sintering, 53, (2021) 1-8.
4. L. Urtekin, A. Genç, F. Bozkurt, MTAEC9, 53(5), (2019) 619-625.
5. L.Urtekin, A.Taşkın, Materials Express, 7(4), (2017) 245-252.
6. L.Urtekin, F. Bozkurt, M. Canli, Journal of Materials Research and Technology, 14, (2021) 277-286.
7. W. Liu,X.Yang,Z. Xie, et al. Journal of the European Ceramic Society,32(10), (2012) 2187-2191.
8. D. F.Heaney, Handbook of metal injection molding, Elsevier, (2012) 15-65.
9. H.Y. Valera, S.N.Bhavsar, Procedia Technology,14 (2014) 528-534.
10. K.S. Sangwan, S. Saxena, G. Kant, Procedia CIRP, 29 (2015) 305-310.
11. O. Abouelatta, J. Mádl, Journal of Materials Processing Technology, 118 (2001) 269-277.
12. Y. Guo, Y. Wang, B. Gao, et al., Ceramics International, 42(15) (2016) 16729-16737.
13. Z. Guoge, R.S. Chandel,Journal of Materials Science, 40 (7), (2005) 1793-1796.
14. X. Shao, X. Guo, Y. Han, et al., Materials & Design, (1980-2015) 1001-1010.
15. H. Somekawa, K.Higashi, Materials Transactions, 44(8) (2003) 1640-1643.
16. C. Li, Q. Huang, P. Zhang, Journal of Nuclear Materials, 386-388 (2009) 550-552.
17. O.M. Akselsen,Journal of Materials Science, 27(3) (1992) 569-579.
18. M.F. Ashby,Acta Metallurgica, 22(3) (1974) 275-289.
19. D.S. Wilkinson, M.F. Ashby,Acta Metallurgica, 23(11) (1975) 1277-1285.
20. J. Zhang, Y. Huang, Y. Liu, et al.,Materials & Design, 137 (2018) 473-480.
21. Q. Cai, W. Liu, Z. Zhao, Fusion Engineering and Design, 125 (2017) 189-194.
22. J. Lemus-Ruiz, L. Ceja-Cárdenas, J.A. Verduzco, Journal of Materials Science, 43(18) (2008) 6296-6300.
23. A. Safarian, M. Subaşı, Ç. Karataş, The International Journal of Advanced Manufacturing Technology, 89(5) (2017) 2165-2173.
24. H. Koçak, M. Subaşı, Ç. Karataş, Ceramics International, 45(17, Part A) (2019) 22331-22335.
25. M. Subaşı, Journal of Manufacturing Processes, 58 (2020) 706-711.
26. M. Dourandish, A. Simchi, E. Tamjid Shabestary, et al., Journal of the American Ceramic Society, 91(11) (2008) 3493-3503.
27. V. Firouzdor, A. Simchi, Journal of Composite Materials, 44(4) (2009) 417-435.
28. J.L. Johnson, L.K. Tan, P. Suri, JOM, 55(10) (2003) 30-34.
29. T. Li, Q. Li, J.Y.H. Fuh, International Journal of Refractory Metals and Hard Materials, 27(1) (2009) 95-100.
30. M. Subaşı, K. Samet, Ç. Karataş, GU J Sci, Part C, 8(2) (2020) 475-485.
31. G.Q. Wu, Z.F. Li, G.X. Luo, Modelling and Simulation in Materials Science and Engineering, 16(8) (2008) 085006.

32. Y. Huang, N. Ridley, F.J. Humphreys, Materials Science and Engineering: A, 266(1) (1999) 295-302.
33. G. Garmong, N.E. Paton, A.S. Argon,Metallurgical Transactions A, 6(6) (1975) 1269-1279.
34. J. Varmazyar, M. Khodaei, Journal of Alloys and Compounds, 773 (2019) 838-843.
35. A.A. Shirzadi, A. Laik, R. Tewari, Materialia, 4 (2018) 115-126.
36. H. Pan, B. Liu, Y. Guo, Materials Letters, 240 (2019) 185-188.
37. D. Wang, J. Cao, W. Li, International Journal of Hydrogen Energy, 42(9) (2017) 6350-6359.
38. R.R. Wang, G.E. Welsch, O. Monteiro, J Biomed Mater Res., 46(2) (1999) 262-270.
39. M.G. Nicholas, R.M. Crispin, Journal of Materials Science, 17(11) (1982) 3347-3360.
40. L.M. Zhao, Z.D. Zhang, Scripta Materialia, 58(4) (2008) 283-286.

Сажетак: *Метода бризгања праха (ПИМ) се широко користи у производњи делова сложене геометрије и малих запремина. Да би се решило ограничење запремине у ПИМ-у, развијена је метода уметнутог бризгања праха (ИПИМ). У овој студији, утицај храпавости површине уметка на чврстоћу на смицање испитан је применом ове методе у производњи WC-9% Co делова. Прво су од челика 4340 за истраживање припремљени уметци са пет различитих површинских храпавости (Ra, μm), 1.5 - 2.1 - 3.3 - 4 - 4.6. WC сировина је убризгана на припремљене уметке. Након процеса инјектирања, узорци су подвргнути процесима растављања и синтеровања. Испитивања компресије су изведена на синтерованим узорцима и испитиван је утицај храпавости површине на чврстоћу дифузионог везивања. Као резултат експеримената, утврђено је да чврстоћа смицања расте са повећањем храпавости површине уметка. Максимална чврстоћа на смицање (118,4 MPa) добијена је у узорцима са храпавостом површине уметка од 4,6 μm.*

Кључне речи: *Уметнуто бризгање праха, чврстоћа површине, дифузионо везивање, смицање, WC сировина.*